An Automated Visualization System for Pulmonary Blood Flow Assessment using Non-Contrast Enhanced and Contrast Enhanced CT Images

Shoji Kido[1], Hidenori Shikata[2], Yoshitaka Tamura[3], Kazuo Awai[3], and Yasuyuki Yamashita[3]

[1] Applied Medical Engineering Science, Yamaguchi University Graduate School of Medicine, Japan, kido@ai.csse.yamaguchi-u.ac.jp
[2] Ziosoft Inc., CA, USA,
[3] Diagnostic Radiology, Graduate school of Medical Sciences, Kumamoto University, Japan

Abstract. Contrast enhanced (CE) CT images are commonly used for pulmonary embolism (PE) detection and blood flow assessment. The enhancement by the contrast medium introduces an intensity difference in the regions with and without sufficient blood flow. By the difference, thrombus can be visually recognized as a region with no enhancement in CE CT images. In parenchyma region, the enhancement can also be observed in the regions with normal blood flow. However, it is only subtle, causing difficulties in differentiating the regions with low blood flow. In order to assist blood flow evaluation in parenchyma region as well as in vessel, we have developed an automated visualization system that generates color-coded subtraction images between non-CE CT images and CE CT images via non-rigid registration. The subtraction images produced by the system resemble to the image obtained from blood flow scintigraphy SPECT scan, which shows clinical importance of this system by its potential ability to enable blood flow assessment with only CT images.

Keywords: Registration-2D/3D, Computer Assisted Diagnosis, Functional Imaging, Quantitative Image Analysis

1 Introduction

Blood transports substances to support cellular activities through blood vessels. Any blockages in a vessel lead to the lack of blood supply to the region covered by the subsequent vessel subtrees, which may cause severe symptoms. Such obstructions must be detected and treated in their early stage. Pulmonary embolism (PE) is a typical disease that prevents blood flow. The number of PE patients are increasing annually and the mortality rate is high [1]. For PE detection, contrast enhanced (CE) CT images are commonly used in clinical practice. Intensity values in CE CT images increase significantly compared with non-CE CT images in vessels with normal blood flow. The enhancement makes noticeable difference between a vessel and a thrombus,

which enables the thrombus to be visually recognized in the image. There are several systems that support PE detection such as in [2]. These systems are potentially able to detect subsegmental PEs those are difficult to identify by visual inspection. However, the systems are not usable for regional blood flow assessment in parenchyma.

The radii of the pulmonary vessels decrease along bifurcations to the periphery. In the capillary bed, blood flows from the pulmonary artery into vein. Though the peripheral vessels are well under CT resolution, the function can be noticed by the increase of CT value in CE CT images. Therefore, if there is any blockage in a vessel and blood flow decreases, low or no enhancement in the parenchyma region covered by the subsequent subtree is likely to be observed. It is clinically important to identify the region with low blood flow both for understanding severity and treatment planning. In parenchyma region, intensity increases by approximately 30-50 HU in normal case, whereas 100 HU or more enhancements can be observed in vessel. Due to the low contrast, it is relatively difficult to identify parenchyma region with low blood flow if only CE CT images were available.

In order to evaluate blood flow in parenchyma region, blood flow scintigraphy with SPECT image is useful. In blood flow scintigraphy, radioisotope (RI) is injected as maker and the SPECT scanner visualizes its distribution. Since pulmonary vessels spread in the entire lung, the distribution of the maker can be interpreted as the distribution of blood flow. Though the SPECT image cannot visualize anatomical structures by itself, CT-SPECT image fusion augments the missing information and the fusion image can improve diagnosis based on SPECT images [3, 4]. However, it is not well suited for evaluating local blood flow primarily due to the low spatial resolution.

In order to assist blood flow assessment in parenchyma region as well as in vessel, we have developed an automated visualization system that generates color-coded subtraction images between non-CE CT images and CE CT images via non-rigid registration. Advantages of this system are listed as follows;

a. The system can be used for the assessment of blood flow distribution in parenchyma region as well as PE detection.
b. The system uses only CT images that have high spatial resolution and ability to depict anatomical structures.
c. The system uses only CT images that are more commonly used than SPECT images. In addition, the management of the contrast medium is easier than RI, which may contribute to establish cost-effective blood flow evaluation method.

2 Method

The proposed system consists of three steps, preprocessing, registration and subtraction. In the preprocessing step, pulmonary vessels and lung region are extracted to form masks to be used in the following registration and subtraction steps. Registration is performed with a free-form deformation model based on B-spline. Subtraction images are generated using vessel segmentation result. The subtraction

images are color-coded and overlaid onto original CT images. Details can be found in the following subsections.

2.1 Preprocessing

Pulmonary vascular tree and lung segmentation are performed in this step. Vessels are automatically extracted from both non-CE and CE CT images based on the method in [5]. Segmentation process is as follows; Segmentation of the pulmonary vascular trees is performed by applying a combination of an adaptive Gaussian filtering and a vessel traversal. With cylindrical vessel model, the intensity values at the points inside the model decrease after applying Gaussian smoothing. Using the model, a voxel is marked as vessel point when the CT value at the voxel lowered after convolving Gaussian function with an appropriate standard deviation. A set of Hessian matrices and their eigenvalues / eigenvectors are calculated at the same time in order to determine if the voxel is close to the vessel centerline. A set of points that are close to the centerline is used as seed points for the following vessel traversal to construct connected vascular trees and to eliminate noise elements. Starting from a seed point, the traversal front position is updated by progressing toward a tangent direction approximated by an eigenvector of the Hessian matrix at the point. This process extracts pulmonary vascular trees without user interaction.

Lung region is extracted by a combination of global threshold and morphological operations. After the lung segmentation, two volumes of interest (VOIs) that tightly cover the left and the right lung are set to extract each lung. The volume of each VOI is approximately 1/4 of the original volume.

2.2 Registration

The registration for this specific application can be described as an intra-subject, mono-modality registration with non-rigid deformation and intensity alteration between the images. Lung surface moves smoothly on pleura during the respiration and that causes abrupt non-rigid deformation between two different CT scans in terms of the relative spatial distance between the structures in body, namely ribs, and the internal lung structures. The deformation often lowers registration accuracy in lung periphery when using a smooth deformation model. Therefore, the lung mask is applied to exclude structures outside the lung. The masked CT images that contain only lung region are used as input for the registration.

The height of an adult human lung with full inspiration is about 25-30 cm and a whole lung scan typically includes 300-350 slices with 1 mm slice thickness. Using whole volume for registration requires massive computational cost. In many applications, subsampled images are used to avoid the problem. Though registration with subsampled images provides visually good results, higher registration accuracy will improve the quality of the subtraction images. We therefore employed a multi-resolution registration approach [6] using automatically extracted two VOIs that include the left and the right lung separately. The first registration is performed using subsampled non-CE and CE CT images by factor of 2. Then the secondary

registration is applied independently to the left and the right lung with the original resolution. This reduces memory consumption per process and the secondary registration can be performed in parallel.

In the registration, a free-form deformation based on B-spline [7] is used as deformation model and mutual information [8] is used as similarity measure. In each resolution level, CT values are converted into 64 bins and the maximum of 50 iterations are allowed for the massive computational cost. We defined 64 bins by dividing equally the difference between maximum and minimum CT values of the lung region into 64 steps. The registration program was written using Insight Segmentation and Registration Toolkit (ITK).

2.3 Subtraction

While the registration in the previous step yields highly accurate registration results, the registered image will have some extent of misalignment. Simple subtraction of the intensities between the corresponding points includes errors introduced both by registration and interpolation. Smoothing is a way to possibly reduce the direct effect of the errors. However, taking mean value of all neighboring voxels without distinguishing vessel and parenchyma is likely to introduce additional error since the extent of the enhancement is different between these two regions. Therefore, the source values of the subtraction are calculated as mean of neighboring vessel points or non-vessel points depending on the location. If a voxel is on a vessel point, the mean intensity of all vessel points among the neighboring voxels is used for subtraction. Similarly, if a voxel is on a non-vessel point, the mean intensity of all non-vessel points among the neighboring voxels is calculated. When a point is on vessel (non-vessel) point and no vessel (non-vessel) points were available in the neighbor, the point is excluded from taking subtraction. The vessel segmentation result for both non-CE CT image and CE CT image are available to distinguish the non-vessel points and the vessel points. This process possibly relaxes registration errors and contributes to provide smooth subtraction images. We empirically used a cubic VOI of $7 \times 7 \times 7$ voxels to define neighboring voxels.

3 Results

The proposed system was applied to 10 sets of non-CE and CE CT scans from 10 patients and the color-coded images were generated for each case. All scans were acquired by a 40-slice multi-detector row CT scanner. Each image consisted of 512×512 pixels and the pixel dimension was about $0.6\ mm^2$. Slice thickness was 1mm and approximately 300-350 slices were available per scan.

In the preprocessing step, it is visually confirmed that the vessel and lung segmentation were successfully performed for all cases ($10 \times 20 = 20$ scans), and the separation into the left and the right lung were also performed without failure.

Followed by the preprocessing step, the multi-resolution registration was performed. The registration takes approximately 15 minutes in each level with a PC

that equips a Pentium 4 3.0 GHz and 2 GB RAM, resulting in 45 minutes for total registration. After the registration, simple subtraction from the deformed CE CT image to non-CE CT image was taken for evaluating registration results. Please note that this simple subtraction was taken for evaluation purpose only and is different from the way to produce final subtraction images as explained in Section 2.3. Since the intensities are to increase in most of the locations in CE CT images, negative values after the subtraction, especially at vessel point, imply misalignment. Therefore, we counted the number of vessel points whose subtraction value is negative as a measure to evaluate the registration.

Table 1 shows the ratio between the number of negative points and the total number of vessel points. For comparison, two additional registration results are also shown in the table. Method 1 used subsampled, nopreprocessed CT images as input and up to 500 iterations were allowed. Method 2 used subsampled, lung masked CT images and up to 500 iterations were allowed. Method 3 is the multi-resolution registration used in our experiments. It took approximately 45 minutes per case for all three methods. The figures in the table show that the multi-resolution approach significantly reduced the number of negative points for all cases. The result indicates better registration with the multi-resolution method.

Table 1 Percentage of the negative voxels in the vessel mask

	Method 1 (%)	Method 2 (%)	Method 3 (%)
case 1	41.1	21.7	11.6
case 2	27.8	15.3	9.3
case 3	18.9	12.0	6.5
case 4	21.3	10.6	5.4
case 5	22.2	12.0	7.8
case 6	29.5	21.8	13.6
case 7	23.7	17.3	11.8
case 8	28.3	20.1	11.2
case 9	33.9	21.0	13.4
case 10	22.9	15.7	14.5

In order to visualize the voxels with negative subtraction value, volume rendering images obtained from case 2 are shown as an example in Figure 1. In the Figure 1(a) and (c), a low opacity value was assigned to the voxels whose subtraction value is in the range from 100 to 250, which infer well aligned vessels. In (b) and (d), voxels with negative value were overlaid on (a) and (c) with a brighter color. The figure shows that the negative value were observed most around the lobular fissures and the

diaphragm pointed by the white arrows, indicating that special care may be needed in these regions to obtain more registration accuracy.

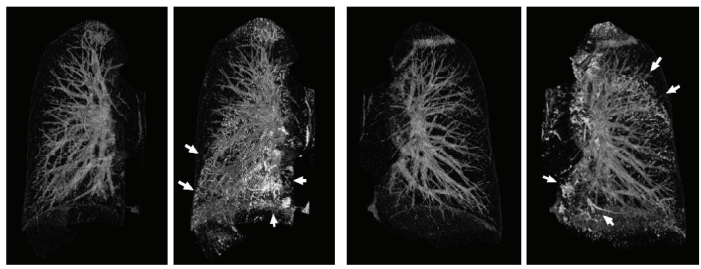

Fig. 1 Volume rendered images of the simple subtraction images after the registration. (a) and (c) visualize voxels whose subtraction values ranging from 100 to 250 in grey color, indicating well aligned vessels.(b) and (d) visualize negative voxels after subtraction in a brighter color, indicating potential misalignment.

Figure 2 shows two examples of the final output, color-coded subtraction images and corresponding RI-SPECT images. The RI-SPECT images available for this study had $64 \times 64 \times 64$ voxels in size and voxel dimension was $6.4\,mm^3$. The RI-SPECT image was manually registered and overlaid onto the corresponding CT image with a colormap shown in each figure. Blue and red colors denote low and high blood flow, respectively. In Figure 2, (a) and (c) are RI-SPECT images and (b) and (d) show the subtraction images generated by the system. In Figure 2, (a) and (b) show a case which shows a defect region of pulmonary blood flow in right lung (case 1). (c) and (d) show a case which shows a defect region of pulmonary blood flow in right upper lung (case 2).

In case 1, a defect region of pulmonary blood flow in the right lung was indicated by a red arrow in RI-SEPCT image (a). The subtraction image shown in (b) also rendered the similar region with the same color. However, the defect region of pulmonary blood flow in subtraction image is smaller than that of RI-SPECT image. In RI-SPECT image, the defect region of pulmonary blood flow is visualized by obstruction of peripheral pulmonary arteries caused by Tc-99mMAA. However, subtraction image suggests that pulmonary blood flow exists in the defect region of RI-SPECT image. This indicates some pulmonary arteries are not obstructed completely. In case 2, (c) shows pulmonary blood flow is extremely low in most of the upper lobe of the right lung. However, the subtraction image in (d) suggests that pulmonary blood flow exists in same region. Also this image indicates defect region of pulmonary blood flow exists in left lung. This is not indicated by RI-SPECT image.

Figure 3 shows two examples that illustrate an airway and a vessel appeared in blue color. In (a), an occluded airway and a vessel run in parallel near a large bronchogenic carcinoma pointed by a yellow arrow. They can be clearly distinguished by the difference of the overlapped color. We can also evaluate activity of obstructive pneumonia caused by bronchogenic carcinoma. In (b), a vessel with nearly no blood flow was shown in blue. So, we can easily evaluate the existence or nonexistence of blood flow.

The Figure 2 and 3 show that the subtraction images produced by the system can support blood flow assessment in both parenchyma and vessels. The availability of the high spatial resolution is an advantage over RI-SPECT image for evaluating local blood flow.

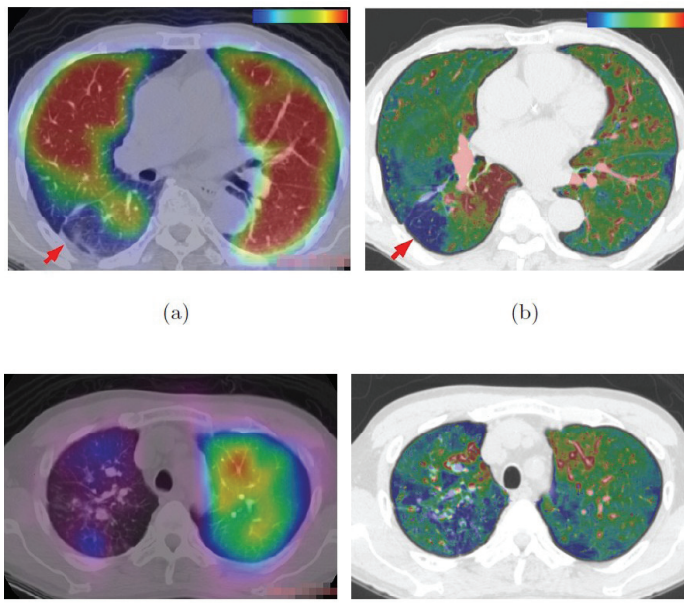

(a) (b)

(c) (d)

Fig. 2 Examples of the color-coded subtraction images that show low blood flow in parenchyma region. (a) and (c) are RI-SPECT images manually registered on the corresponding CT images. (b) and (d) are the subtraction images produced by our system.

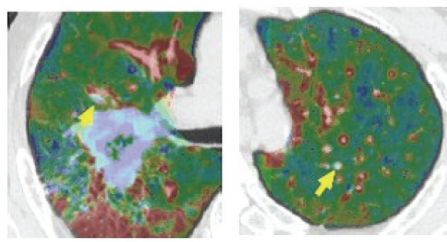

(a) (b)

Fig. 3 Examples of the color-coded subtraction images that depict an airway and a vessel with no blood flow. (a) shows an occluded airway and (b) shows a vessel with nearly no enhancement.

3 Concluison

In this paper, we presented an automated visualization system for spatial assessment of pulmonary blood flow using non-CE and CE CT images. In the clinical practice, blood flow in vessel is evaluated with CE CT images and RI-SPECT images are used for blood flow assessment in parenchyma region. The proposed system can be used for both purposes. In many hospitals in Japan, we can not obtain RI-SPECT images easily, and costs of RI-SPECT study are high. However, our system uses only CT images, which may reduce the overall diagnosis time and cost. Moreover, our system may add more information about pulmonary blood flow to that of RI-SPECT study. The future task includes the development of an algorithm to detect the low blood flow region and PE from the images generated by our system.

Acknowledgements

This work was supported in part by the Grant-in-Aid for Scientific Research on Priority Areas (15070208) from the Ministry of Education, Culture, Sports, Science and Technology, Japan.

References

1. Schoepf, U.J.: Diagnosing pulmonary embolism: time to rewrite the textbooks. The International Journal of Cardiovascular Imaging 21, 155-163 (2005)
2. Masutani, Y., MachMahon, H., Doi, K.: Computerized detection of pulmonary embolism in spiral CT angiography based on volumetric image analysis. IEEE Transactions on Medical Imaging 21, 1517-1523 (2002)
3. Gutman, F., Hangard, G., Gardin, I., Varmenot, N., Pattyn, J., Clement, J.F., Dubray, B., Vera, P.: Evaluation of a rigid registration method of lung perfusion SPECT and thoracic CT. American Journal of Roentgen logy 185, 1516-1524 (2005)
4. Suga, K., Kawakami, Y., Iwanaga, H., Seto, A., Matsunaga, N.: Comprehensive assessment of lung CT attenuation alteration at perfusion defects of acute pulmonary thromboembolism with breath-hold SPECT-CT fusion images 185, 1516-1523 (2005)
5. Shikata, H., Hoffman, E.A., Sonka, M.: Automated segmentation of pulmonary vascular trees from 3D CT images. In:Proc. SPIE, San Diego, USA (2004)
6. Schnabel, T., Rueckert, D., Quist, M., Blackall, J.M., Castellano-Smith, A.D., Hartkens, T., Penney, G.P., Hall, W.A., Liu, H., Truwit, C.I., Gerritsen, F.A., Hill, D.L.G., Hawkes, D.J.: A generic framework for nonrigid registration based on nonuniform multi-level free-form deformations. In: Lecture Notes in Computer Science (MICCAI 2001) 2208, 573-581 (2001).
7. Rueckert, D., Sonoda, L.I., Hayes, C., Hill, D.L.G., Leach, M.O., Hawkers, D.J.: Nonrigid registration using free-form deformations: Application to breast MR images. IEEE Transactions on Medical Imaging 18, 712-721 (1999)
8. Mattes, D., Haynor, D.R., Vesselle, H., Lewellen, T.K., Eubank, W.: PET-CT image registration in the chest using free-form deformations. IEEE Transactions on Medical Imaging 22, 120-128 (2003)